PNAS
www.pnas.org

Supplementary Information for

In vitro reconstitution reveals phosphoinositides as cargo-release factors and activators of the ARF6 GAP ADAP1

Christian Duellberg, Albert Auer, Nikola Canigova, Katrin Loibl and Martin Loose

Christian Duellberg and Martin Loose

Email: Christian.duellberg@ist.ac.at and martin.loose@ist.ac.at

This PDF file includes:

Supplementary methods
Figures S1 to S7
Table S1
Legends for Movies S1 to S4
SI References

Other supplementary materials for this manuscript include the following:

Movies S1 to S4

Supplementary Methods

Protein purification

The cDNA for mouse full length ADAP1 (UniProtKB - E9PY16) was codon optimized (OptimumGene, Genscript) for SF9 insect cells, synthesized by Genscript and subcloned into a pFastBac HTb vector (Invitrogen/Thermo Fischer), from which Baculoviruses were generated. For fluorescent ADAP1, *Clavularia* derived mWasabi (GenBank:EU024648.1) was codon optimized for insect cells, synthesized by Genscript and cloned in front of ADAP1, separated by a GGGGG linker. Phusion HF polymerase (NEB) was used for all cloning steps. mWasabi was chosen because of its monomeric nature and bright fluorescence (1). For ADAP1-6xHis, a hexahistidine tag was cloned between the ORF and the stop codon without a linker. Cells were harvested 72 hours after infection and were maintained at 27° C in ESF medium (Oxford Expression Technologies) supplemented with 0.1 mM $ZnCl_2$ (Sigma) during protein production. Cells were lysed in 20 mM Tris-HCl (pH 8.0), 300 mM KCl, 3mM $MgCl_2$, 5mM 2-mercaptoethanol supplemented with DNAse I (Sigma) and cOmplete EDTA free Protease Inhibitor Cocktail tablets (Roche) using a glass homogenizer. Protein in clarified lysates was bound to Protino-TED resin (Macherey-Nagel), washed with ~ 100 ml wash buffer (20mM Tris-HCl (pH 8.0), 300 mM KCl, 1mM $MgCl_2$, and 5mM 2-mercaptoethanol) and eluted with wash buffer supplemented with 400 mM imidazole. Eluted protein was immediately buffer exchanged into wash buffer using PD10 desalting columns (GE Healthcare) because long incubation times with imidazole can unfold zinc finger domains (2). Aminoterminal hexahistidine tags were cleaved by TEV protease at 4° C. The protease and the cleaved hexahistidine tags were removed by passing the protein solution through a Ni-TED column and ADAP1 was recovered from the flow through. Proteins were gel filtered in wash buffer using a Superdex 200 column (GE Healthcare). Pure fractions were pooled (SI Appendix, Fig. S6), aliquoted, snap frozen in liquid N_2 and stored at – 80 °C.

The cDNA for mouse KIF13B (Uniprot KB-E9Q4K7) was codon optimized for insect cells (OptimumGene, Genscript) and synthesized by BaseClear. The coding sequence for amino acids 1-584 were subcloned into a pFastBac HTb vector and used for Baculovirus production. For KIF13B-6xHis, a HIS tag was cloned between the ORF and the stop codon without a linker. Cells were harvested 72 hours after infection and protein purification was performed as described (3). The FHA domain (amino acids 438 – 544) of KIF13B was subcloned into a pET-50 vector (Novagen) and expressed in BL21 cells at 18 °C overnight. Purification was performed as for the longer construct except that C3 protease was used to remove the purification tag.

cDNA for GGA3 (Uniprot KB - Q9NZ52-GGA3 HUMAN) was a gift from Martin Schwartz (Yale School of Medicine, USA) (Addgene plasmid # 18841) (4). Coding sequence for amino acid 146-302 was cloned into pTB146 vector (gifted by Thomas Bernhardt, Harvard Medical School, Boston, USA) and expressed as a 6X histidine sumo fusion protein in BL21 cells at 18 °C overnight in TB medium (Terrific Broth) in the presence of 400 µM Isopropyl-β-D-thiogalactopyranosid (IPTG). Cells were lysed using a glass homogenizer and sonication in 50mM HEPES (pH 7.4), 300 mM KCl, 3mM $MgCl_2$, 0.1% Nonident P-40, 5mM 2-mercaptoethanol, 1 tablet of protease inhibitor and DnaseI. Protein in cleared lysates was bound to Protino-TED resin, washed with ~ 100 ml wash buffer (50mM HEPES (pH 7.4), 300mM KCl, 3mM $MgCl_2$, 0.1% Nonident P-40, 5mM 2-mercaptoethanol) and eluted with wash buffer supplemented with 350 mM imidazole. Imidazole was removed using PD10 desalting columns and the purification tag was cleaved using ULP1 protease at 4 °C overnight and removed by passing the solution through a Protino-TED column. Protein was gel filtered using a Superdex 75 column (GE Healthcare) in gel filtration buffer (HEPES (pH 7.4), 300mM KCl, 3mM $MgCl_2$, 5mM 2-mercaptoethanol). Pure fractions were pooled (SI Appendix, Fig. S6), aliquoted, snap frozen in liquid N_2 and stored at – 80 °C.

cDNA for yeast NMT1 (UniprotKB- P14743-NMT YEAST) was a gift from Marc Kirchner and subcloned into a pETDuet1 vector (Novagen) with an N terminal 6X histidine tag. NMT1 was overexpressed in BL21 cells at 18 °C overnight in TB medium in the presence of 400 µM IPTG. Cells were lysed in 20mM sodium phosphate buffer (pH 7.3), 500 mM NaCl, 3 mM $MgCl_2$, 10mM 2-mercaptoethanol, 1 tablet of protease inhibitor and DNase I using a glass homogenizer and sonication. Protein in cleared lysates was bound to Protino-TED beads, washed with ~ 100 ml wash buffer (20mM NaPi (pH 7.3), 500mM NaCl, and 10mM 2-mercaptoethanol) and eluted with wash buffer supplemented with 350 mM imidazole. Imidazole was removed by PD 10 desalting columns and protein was gel filtered in wash buffer using a Superdex 200 column. NMT1 was used fresh after purification without freezing.
cDNA for ARF6 (aa 2-175 / UniProtKB - P62331) was codon optimized for *E. coli* and synthesized by Integrated DNA Technologies (IDT), cloned into pTB146 vector and expressed as a 6x His sumo fusion protein in BL 21 cells for 4 hours at 37 °C in the presence of 400 µM IPTG. Cells were lysed (20 mM Tris-HCl (pH7.8), 300 mM KCl, 5 mM $MgCl_2$, 5 mM 2-mercaptoethanol, protease inhibitor tablets and DNaseI) by sonication. Protein in cleared lysate was incubated with Protino Ni-TED beads, washed with wash buffer (20 mM Tris-HCl (pH 7.8), 300 mM KCl, 5 mM $MgCl_2$, 5 mM 2-mercaptoethanol) eluted with wash buffer supplemented with 400 mM imidazole and dialyzed into wash buffer in the presence of ULP1 protease to cleave off the His sumo tag. Cleavage reactions were performed overnight at 4 °C. ULP1 and the tag were removed by passing the solution through a Ni NTA column (Thermo) and the protein was gel filtered using a Superdex 200 column. *In vitro* myristoylation was performed and monitored as described (5, 6) except that no ammonium precipitation was performed, because the reaction was complete, as shown in SI Appendix Fig. S7. All purification steps were performed on ice/ in a cold room unless stated otherwise and protein concentrations were determined by Bradford (BioRad) against a BSA standard solution. Absorbances were measured at 595 nm on a Spectramax Me2 plate reader (Molecular Device) at room temperature. Protein identities were confirmed with specific antibodies using standard western blot procedures and commercial antibodies or trypsin digest followed by mass spectrometry. Plasmids will be made available on Addgene.
Tubulin (T240-A), Biotin-Tubulin (T333P-A), Hilyte647-Tubulin (CYS-TL670M-A-5) and X-Rhodamine-tubulin (TL620M-A) were purchased from Biozol Cytoskeleton INC.

Sortase labeling
To generate fluorescent KIF13B, heptapeptides (CLPTEGG) were synthesized (Biomatik) and incubated with CF-488A maleimide dye (Sigma) in a 1:3 ratio in 50 mM HEPES (pH 7.5) and 57 mM TCEP overnight. Reactions were quenched by the addition of 2-mercaptoethanol (1.4 M). Protein and labeled peptide were mixed in a 1:10 ratio and calcium-independent sortase enzyme (7) was added to a final concertation of 10 µM. After 5 hours at 37 °C excess dye/peptide was removed by gel filtration using a Superdex 200 column (GE Healthcare) and proteins were pooled and snap frozen in liquid N_2.

Analytical gel filtration
Proteins were buffer exchanged into gel filtration buffer (20 mM Tris-HCl (pH 7.25), 150 mM KCl, 1 mM $MgCl_2$, 5 mM 2-mercaptoethanol and 0.1 mM ATP,) using Zeba spin columns and loaded onto a Superdex 200 column (GE Healthcare) at a concentration of 2.2 µM. The flow rate was 0.05 ml per minute. The absorbance was recorded at 280 nm. All steps were performed at 4 °C. This experiment was performed in triplicate and one representative example for each condition is shown in SI Appendix Fig. S1B.

Size exclusion chromatography-multi-angle light scattering (SEC-MALS)
40 µg (100 µl of a 9.3 µM solution) purified ADAP1 was resolved on a Superdex 200 in PBS buffer (11. 8 mM NaPi (pH 7.4), 2.7 mM KCl, and 137 mM NaCl) at a flow rate of 0.4 ml per minute at room temperature. Light scattering was recorded on a miniDawn light scattering device (Wyatt) and the change in refractive index was used to define the peak area that was used to obtain the molecular mass. Analysis was performed using Astra software. The mass shown in SI Appendix Fig. S1A is the average of two independent runs.

Vesicle pelleting assay
Lipids were obtained from Avanti lipids and dissolved in chloroform except for PIPs which were dissolved in chloroform, methanol and water (60:33:7). Control vesicles (no PIP) contained 80% DOPC and 20% DOPS. For PIP_3 containing vesicles, DOPS was substituted by PIP_3. Lipids were mixed and dried using streams of inert gas (N_2 or argon) and desiccation. Dried films were resuspended in sucrose containing buffer (20mM HEPES (pH 7.4), 180 mM sucrose, 1mM $MgCl_2$). After multiple freeze-thaw cycles using dry ice and a room temperature water bath, vesicles were extruded (Liposofast extruder / Biopharma / pore size was 400 nm) and directly used for experiments. Vesicles of different PIP_3 contents (total lipid concertation was always 375µM) and ADAP1 (final concentration was 1 µM) were mixed in sedimentation buffer (20mM HEPES (pH 7.4), 180mM NaCl, 1mM $MgCL_2$ and 2mM 2-mercaptoethanol), incubated for 10 minutes and centrifuged for 45 min at 90,000 rpm in a TLA 100 rotor (Beckman) at 23 °C. Pellets were resuspended in buffer, and mixed with SDS loading buffer. 12.5 % of the total supernatant and 50 % of the total resuspended pellet was loaded and resolved on a 12% SDS gel and stained with Coomassie-Brilliant Blue (CBB). Therefore, a correction factor of 4 was applied for the quantifications shown. Gel bands were analyzed using the gel analyzer software. Each PIP_3 concentration was measured in duplicates. For experiments that included KIF13B (SI Appendix, Fig. S2B), ADAP1 was present at 1.1 µM and KIF13B was present at 1 µM. Presented data come from 3 independent experiments.

Quartz Crystal Microbalance with Dissipation (QCMD)
QCMD measurements were performed essentially as described (8). In brief, SiO2-coated sensors (Quartz Crystal5 MHz, AT cut, Gold electrode with Silicon 84 dioxide-coating by Q-Sense) were cleaned in 2% (v/v) SDS and subsequently sonicated in H_2O. Dried and air-plasma activated sensors were mounted into the device (QCMD by LOT-Quantum Design GmbH) and vesicles (100 nm diameter, 100 µg/ml) were flown into the chamber in rapture buffer (20mM Tris-HCl pH 7.8, 300mM KCl, 5mM $MgCl_2$, 5mM 2-mercaptoethanlol, 2mM $CaCl_2$) to form a bilayer. The lipid composition of the vesicles was: 80% DOPC, 20% DOPS and 80% DOPC, 15% DOPS, 5% $PI(3,4,5)P_3$. After washing the bilayer with buffer (20mM Tris-HCl pH 7.8, 300mM KCl, 5mM $MgCl_2$, 5mM 2-mercaptoethanlol), protein was injected in the same buffer at the indicated concertation at a constant flow rate of 20µL/min. All measurements were performed at room temperature.

Microtubule pelleting assay
Microtubules were assembled from tubulin (2.5 mg/ml) in 80mM K-PIPES (pH 6.85), 3.5mM $MgCl_2$, 10mM KCl, 0.5mM GMP-CPP (Jena Bioscience) at 37 °C for 1 hour in a reaction volume of 50µL. Then, 400 µl prewarmed (37 °C) buffer supplemented with 10 µM Paclitaxel (Sigma) without GMPCPP was added and samples were centrifuged at 21,000 g for 9 minutes at room temperature. Pellets were resuspended in 60 µl buffer supplemented with 10 µM Paclitaxel (Sigma). 10 µl microtubules were mixed with ADAP1 (1.3 µM final) and KIF13B (0.7 µM final) in a total volume of 150 µl in the following buffer: 80mM K-PIPES (pH 6.85), 1 mM $MgCl_2$, 35 mM KCl, 0.5 mM AMP-PNP and 10 µM Paclitaxel and centrifuged at 90,000 rpm for 15 min in a TLA 100 rotor (Beckman) at 25 °C. Pellets were resuspended in buffer, and mixed with SDS loading buffer. 10 % of the total

supernatant and 50 % of the total resuspended pellet was loaded and resolved on a 12% SDS gel and stained with CBB. Therefore, a correction factor of 5 was applied for the quantifications shown. Gel bands were analyzed using the gel analyzer software.

mWasabi-ADAP1 intensity along microtubules

Flow chambers assembled from PEG-Biotin glass (9) were washed with buffer (80 mM K-PIPES (pH 6.85), 0.5 mM $MgCl_2$, 10 mM KCl, 2 mM 2-mercaptoethanol, 0.5 mM Adenylyl-imidodiphosphate (AMP-PNP), 12.5 µg/ml β-Casein, 20 mM glucose), buffer supplemented with 0.05 mg/ml Neutravidin (Thermo) and 90 mM KCl, buffer, buffer supplemented with 1 µl GMP-CPP stabilized microtubules (containing ~5% Biotin-tubulin and 5% Hilyte 647 tubulin), buffer, and the final imaging mix (buffer with catalase (0.3 mg/ml), glucose oxidase (0.6 mg/ml), and 160 nM mWasabi- ADAP1). KIF13B (200 nM) was present when indicated and water soluble PI(3,4,5)P3-C4 (Echelon, P-3904 / 23µM), PI(4,5)P2-C4 (P-4504 / 23 µM), PI(3,4)P2-C4 (P-3404 / 23 µM), Inositol 1,3,4,5-tetrakisphosphate (IP4, Sigma, 28 µM) or an equal volume of H_2O (CTL) was present as indicated. Data were recorded on an Olympus IX83 TIRF microscope equipped with a 100X objective at room temperature. For experiments that required solution exchanges (Fig. 2D), flow chambers were fixed with magnets and solutions were exchanged in the flow chamber on the microscope objective. An image was taken before solution exchange and after. The time between solution exchange and capture of the second image was ~ 30 seconds. This data set was recorded on an IMiC TIRF microscope (FEI/TILL photonics, Munich) at room temperature using a 100X 1.49 NA oil objective (Olympus, Japan). Intensity values were obtained from line scan analysis using Image J. Average intensities along the length of a microtubule were background subtracted (intensity of a line in the same image where no microtubule was present) and plotted. For each condition, at least 20 microtubules from 3 independent experiments were analyzed.

Microtubule gliding assays

Microtubule gliding assays were essentially performed as described (10). In brief, KIF13B was diluted in gliding buffer (80 mM K-PIPES (pH 6.85), 1 mM $MgCl_2$, 2 mM 2- mercaptoethanol, 20 mM glucose, 10 mM ATP) to 280 nM and flown into flow chambers assembled from non-functionalized glass coverslips, where motor proteins non-specifically adsorb to glass. After incubation of 7 min, unbound motor was washed out with gliding buffer and final imaging buffer was flown into the chamber (gliding buffer supplemented with 1 µl Paclitaxel stabilized Hilyte 647 labeled microtubules, 0.2 mg/ml β Casein (Sigma) and oxygen scavengers catalase (0.3 mg/ml) and glucose oxidase (0.6 mg/ml) and imaged on a IMiC TIRF microscope (FEI/TILL photonics, Munich) at 30 ◦C using a 100X 1.49 NA oil objective (Olympus, Japan).

Single molecule motility assay

Single molecule experiments were essentially performed as described (10). CF_{488}-KIF13B was present at 10 nM. Imaging buffer was 10 mM K-PIPES (pH 6.85), 35 mM K-Acetate, 1 mM ATP, 12.5 µg/ml β-Casein, 20 mM glucose, 0.3 mg/ml catalase, 0.6 mg/ml glucose oxidase, 2 mM 2-mercaptoethanol and 1 mM $MgCl_2$. For experiments with mWasabi-ADAP1, the PIPES concentration was raised to 40 mM and 20 mM KCl was used instead of K-Acetate to improve solubility of mWasabi-Adap1. Data were recorded on an Olympus IX83 TIRF microscope equipped with a 100X objective at room temperature at framerate of 2 hertz. Run frequencies were obtained from kymograph analysis using image J and were verified manually directly from the movies. Per condition, a total of 10 microtubules from 3 independent experiments were analyzed.

Vesicle motility assay

Dried lipid films containing 89% DOPC, 7% DOPS and 3% DGS-NTA(Ni) and 1% rhodamine-phosphatidylethanolamine or 89% DOPC, 5% DOPS and 5% PI(3,4,5)P3 and 1% rhodamine-phosphatidylethanolamine were reconstituted in vesicle motility buffer (80 mM K-PIPES, 10 mM KCl, 1 mM $MgCl_2$, 1 mM ATP, 2 mM 2-mercaptoethanol, 20 mM Glucose). After five freeze-thaw cycles using dry ice and a room temperature water bath, vesicles were extruded using a Liposofast extruder (Biopharma) with a pore size of 400 nm. HiLyte 647 labeled biotinylated microtubules were attached to PEG-Biotin glass as described above and final imaging buffer (vesicle motility buffer supplemented with 0.3 mg/ml catalase and 0.6 mg/ml glucose oxidase, vesicles (total lipid was 40 µM) and 500 nM KIF13B-His for NTA vesicles or ADAP1 and KIF13B ranging from 10 to 1000 nM for PIP_3 vesicles) was flown into the flow chamber. Fluorescent vesicles were observed on an IMiC TIRF microscope at room temperature using a 100X 1.49 NA oil objective at framerate of 1 hertz. Run frequencies were obtained from kymograph analysis using image J.

End point GAP assay with GGA3 recruitment

Myristoylated ARF6 was loaded with either GTP, GDP or GTPγS as described (6) and buffer exchanged into GAP buffer (20 mM HEPES (pH 7.4), 180 mM NaCl, 2 mM 2-mercaptoethanol) using Zeba Spin desalting columns (Thermo). MyrARF6 (5 µM final) was mixed with GGA3 (5 µM), vesicles (375 µM; vesicles where of 400 nm diameter and their composition was: 49% DOPC, 18.5% DOPS, 30% Cholesterol, 2.5% PIP_3); reconstituted the same way as described under vesicle sedimentation assay), ADAP1 at the indicated concentration or an equal volume of ADAP1 storage buffer and incubated for 1 hour at 37 °C. Samples were centrifuged (90,000 rpm, TLA 100, 45 min) at 23 °C. Supernatants and resuspended pellets were mixed with SDS loading buffer and protein was detected via SDS page and CBB staining.

Determination of nucleotide content

myrARF6 or soluble ARF6 was loaded with GTP or GTPγS as stated above and buffer exchanged into assay buffer (20 mM Hepes (pH 7.4), 180 mM NaCl, 1 mM $MgCl_2$, 2 mM 2-Mercaptoethanol) using polyethersulfone spin concentrators (Thermo). 120 µM ARF6 was then incubated with vesicles (2.5 % PIP_3, total lipid concertation was 400 µM) and either 2 µM ADAP1 or its storage buffer for 100 min at 37 °C. Nucleotides were extracted by successive addition of perchloric acid to a final concentration of 0.6 % (vol/vol) and sodium acetate (final concentration: 260 mM). Precipitated protein and vesicles were removed by ultracentrifugation (300,000 x g, 25 °C, 30 min). The supernatant was filtered (Sartorius Filtrate tubes) and loaded on a Triart S-3 µm C18 HPLC column (YMC Europe) attached to an UltiMate 3000 HPLC system (Dionex). Nucleotides were separated by reversed phase HPLC under isocratic conditions at a flow rate of 150 µl/min. The mobile phase consisted of 100 mM potassium phosphate (pH 6.5), 10 mM tetrabutylammonium bromide and 8 % acetonitrile (vol/vol) at 30 °C. For control experiments, pure nucleotides solutions (GTP (Thermo: R1461, 99% pure), GDP (Sigma, G7127, 96 % pure), GTPγS (Roche, 10220647001, 85 % pure) were diluted in assay buffer to 50 µM and ran under identical conditions as the samples. Absorbance was recorded at 254 nm. For the quantification, the area under each peak was determined with Origin using the multiple peak analyzer function. Experiments with ARF6-GTP were performed in triplicates and controls were performed in duplicates.

Real time kinetics tryptophan fluorescence GAP assay

Myristoylated ARF6 was buffer exchanged into GAP buffer (20mM HEPES (pH 7.8), 180mM NaCl, 1mM MgCl2 and 5mM 2-mercaptoethanol) using Zeba Spin desalting columns. ARF6 and ADAP1 or ADAP1-6xHis were mixed at the indicated concentrations in 96 well plates (UV-star clear bottom plates, Greiner) and the intrinsic tryptophan fluorescence was monitored on a Spectramax Me2 plate reader (Molecular Device) at 37 °C with λ exc = 290nm, λ em = 350. When vesicles (400nm diameter) were present, their concentration was always 375 µM (total lipid concentration) and contained 80% DOPC and 20% DOPS or 80% DOPC, 17.5% DOPS and 2.5% phosphoinositides (PI(3)P, PI(4,5)P_2, PI(3,4)P_2, PI(3,4,5)P_3). For PI(3,4,5)P_3 and DGS-NTA(Ni) titrations vesicles contained 80% DOPC and 20% DOPS, substituting DOPS by PI(3,4,5)P_3 or DGS-NTA(Ni) at the indicated percentage. For experiments that included the FHA domain (Fig. 5D), FHA was present at 10 µM. Each condition was performed at least in triplicates and errors are standard error of the mean.

To quantify kinetics, intrinsic tryptophan decrease was fitted to a mono-exponential decay to extract *Tau* values (1/ λ (decay rate)) and calculate k_{obs} values (63.2% substrate concentration/ *Tau*). Intrinsic Tryptophan decreases which showed only a slow decrease at low PI(3,4,5)P_3 concentrations were fitted to a mono-exponential decay defining a plateau of decay (Y=(Y0 - Plateau)*exp(-K*X) + Plateau) based on the mean of the highest PI(3,4,5)P_3 concentrations at decay-saturation. k_{obs} values versus PI(3,4,5)P_3 concentrations were fitted by a Hill equation to extract the Hill coefficient. k_{obs} values versus ADAP1 concentration were fitted to a linear regression to estimate the catalytic efficiency k_{cat}/K_m from the slope. All k_{obs} values come from three or more experiments and errors are standard deviation. k_{obs} values to extract the catalytic efficiency are based on fitting the mean fluorescence decrease of triplicates.

To estimate K_m, the mean initial linear decrease of triplicates was determined and fitted to a line fit to extract the initial velocity (V_i) from the slope. V_i values versus ARF6 concentrations were fitted to a Michaelis-Menten equation to estimate K_m.

As both, ADAP1 and the FHA domain of KIF13B contain tryptophans, they increased the initial fluorescent signal, essentially creating an offset. We verified that extracted τ values are not affected and introduced various offsets to our data sets and found that τ values did not significantly change. All intrinsic tryptophan raw fluorescence units (RFUs) were normalized by dividing RFUs by the maximum RFU for each individual measurement. As myrARF6 in a GDP state also shows intrinsic tryptophan fluorescence, the normalized data will not reach 0 even after complete hydrolysis of GTP.

Mass spectrometry

Intact mass analysis of myristoylated ARF6 was performed by the Mass Spectrometry Facility (MPL, Vienna) as followed: Protein was reduced in 5mM DTT for 30 min and diluted with H_2O to a concentration of 20 ng/µl. 40ng of protein were loaded onto the Xbridge (Waters) column attached to a nano-LC-MS-system (Dionex /Waters Synapt G2Si) at a flow rate of 300µl/min using a step gradient of 12-40-64% acetonitrile. Average mass was reconstructed using MacEnt1 software.

Protein identities were confirmed by standard methods using SDS gel extraction followed by trypsin digest by the mass spec facility of IST Austria.

Quantification of band intensities in SDS gels

Protein bands in CBB stained SDS gels were quantified using GelAnalzyer (Gelanalyzer.com). Background subtraction was performed in “valley to valley” mode. Plotted values are band intensities after background subtraction. When bands are presented as fractions (SI Appendix, Fig. S2, Fig. 3), values were calculated as Intensity $_{pellet}$ + Intensity $_{supernatant}$ = 1 (=100%) and the relative fraction is plotted. When unequal amounts of pellet and supernatant was loaded, correction factors

were applied for the quantification, as detailed in the section “vesicle pelleting assay” and “microtubule pelleting assay”.

Statistical analysis

Statistical analysis was performed with Excel. To test for statistical significance a two-tailed unpaired t-test, assuming Gaussian distribution and same variance for both populations was used. For the data in Fig. 2 E, a paired T test was used. Statistical significance in the figures is given: N.S: Not significant, * : $p < 0.05$, ** : $p < 0.01$ and *** $p < 0.001$. All p values are summarized in table S1. Displayed box plots encompass the 25–75th percentiles, the midline indicates the median, the whiskers extend to show the rest of the distribution and to indicate outliers.

Software

Figures were prepared in Adobe Illustrator and graphs were generated using Python. Fitting was performed in Python. SDS bands were quantified using GelAnalyzer (www.gelanalyzer.com/). Statistical tests were performed in Microsoft Excel. Fluorescence intensities and velocities from time lapse movies were analyzed using ImageJ. SEC-MALS data were analyzed in Astra and HPLC data were analyzed with Origin lab.

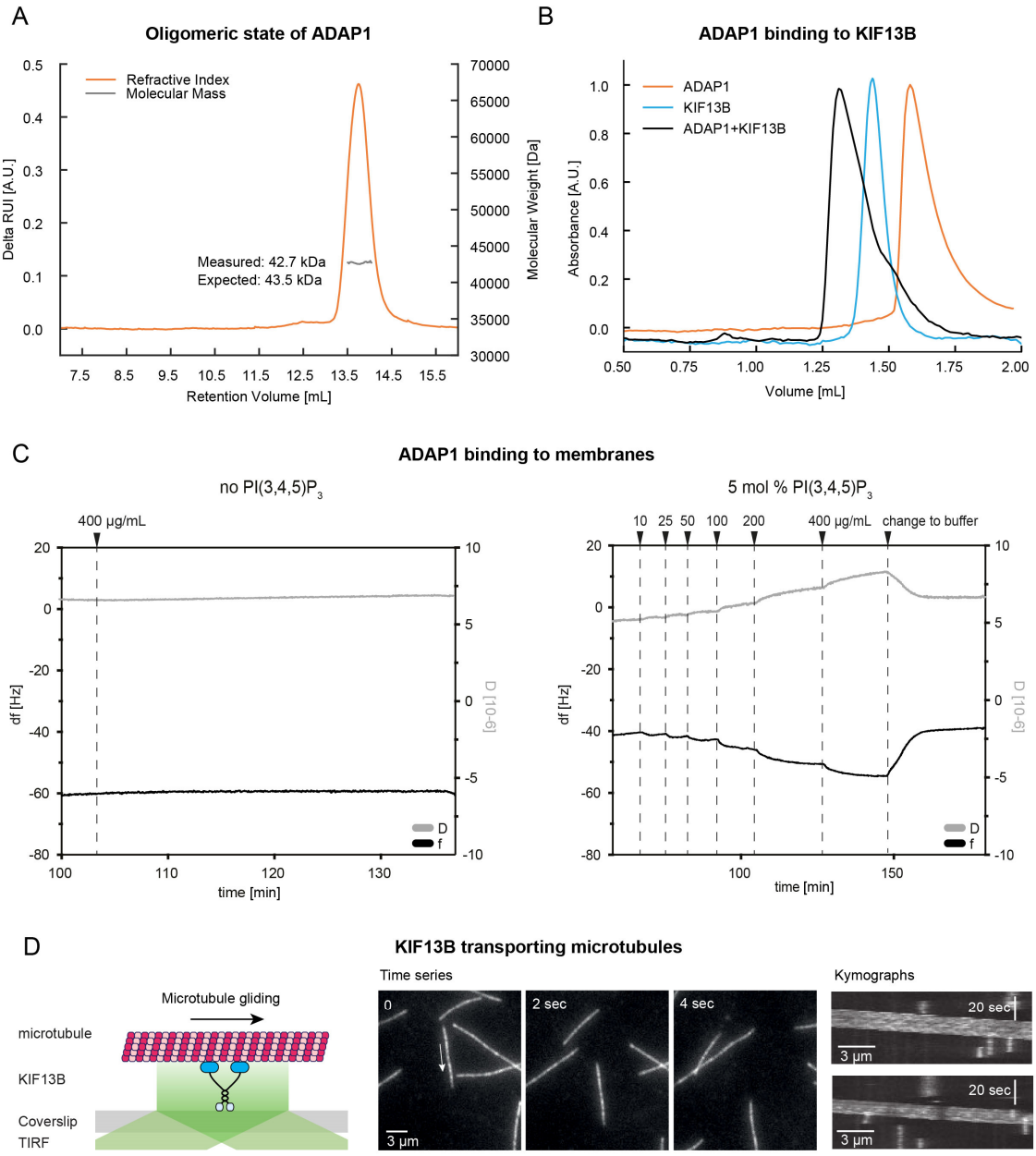

Figure S1: Quality control of proteins and confirmation of published binary interactions
(**A**) Analysis of the oligomeric state of purified ADAP1 by SEC-MALS. Representative trace of the refractive index (orange line) and the corresponding molecular mass obtained from light scattering (grey line). Obtained average mass (inset) is derived from 2 independent experiments and 40 µg ADAP1 was loaded per run. (**B**) Representative analytical gel filtration traces of ADAP1 (orange), KIF13B (light blue) or ADAP1 and KIF13B together (black). Protein concentrations of the injected solutions were 2.2 µM for each protein. (**C**) QCMD traces of change in frequency (f) and dissipation (D) upon binding of ADAP1 to membranes that either have 0 % PIP_3 (left) or 5 % PIP_3 (right). (**D**) Top: Scheme of microtubule gliding assay: Motor protein are adsorbed onto the glass coverslip and transport fluorescently labeled microtubules imaged by TIRF microscopy. Bottom: Time series (left) and two kymographs (right) depicting unidirectional movement of microtubules.

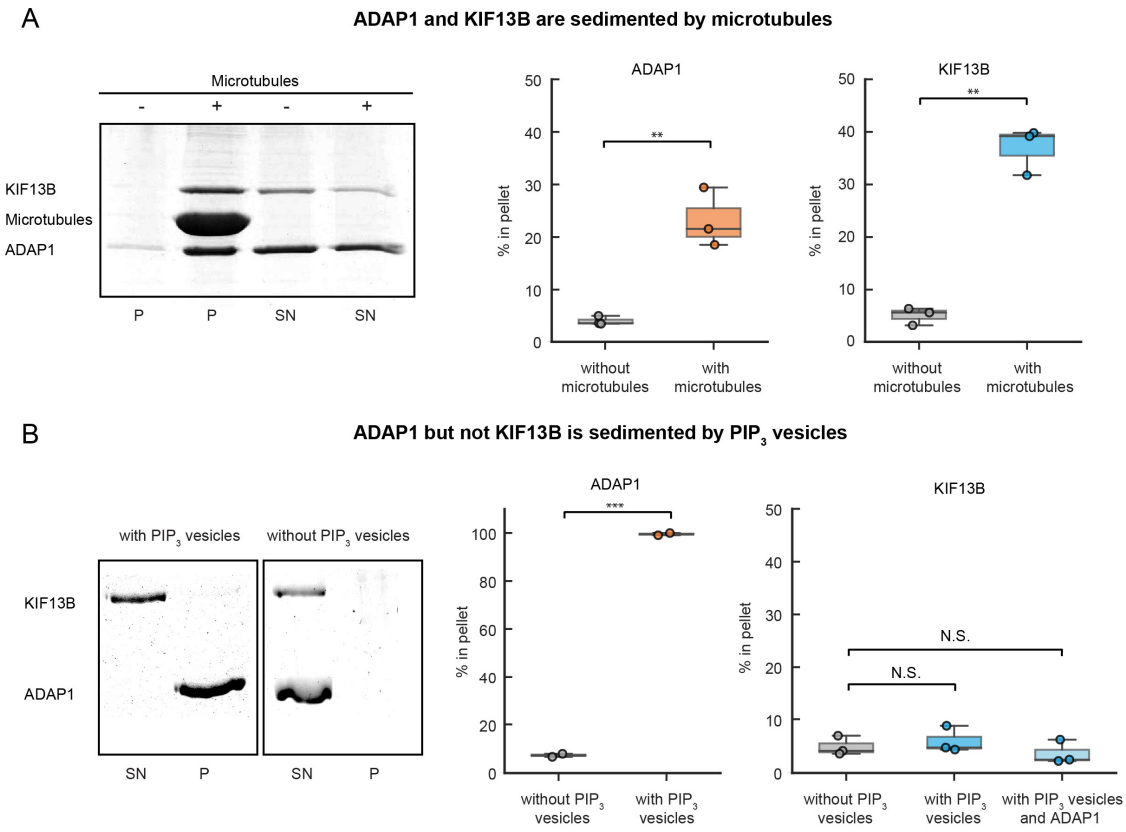

Figure S2: Differential recruitment of ADAP1 and KIF13B by microtubules and PIP3
(A) Left: Representative SDS gel image of pellet and supernatant fractions of ADAP1 and KIF13B after centrifugation in the presence (left) or absence (right) of stabilized microtubules. P = pellet and SN = supernatant. ADAP1 was present at 1.3 µM and KIF13B at 0.7 µM. Right: Quantification of the distribution between supernatant and pellet for ADAP1 (left) and KIF13B (right) based on the SDS band intensity. (B) Left: Representative SDS gel image of pellet and supernatant fractions of ADAP1 and KIF13B after centrifugation in the presence (left) or absence (right) of vesicles containing 2.5 mol % PIP3. ADAP1 was present at 1.1 µM and KIF13B at 1 µM. Note that different amounts of pellet and supernatant are loaded (methods). Quantification of the distribution between supernatant and pellet for ADAP1 (left) and KIF13B (right) based on the SDS band intensity.

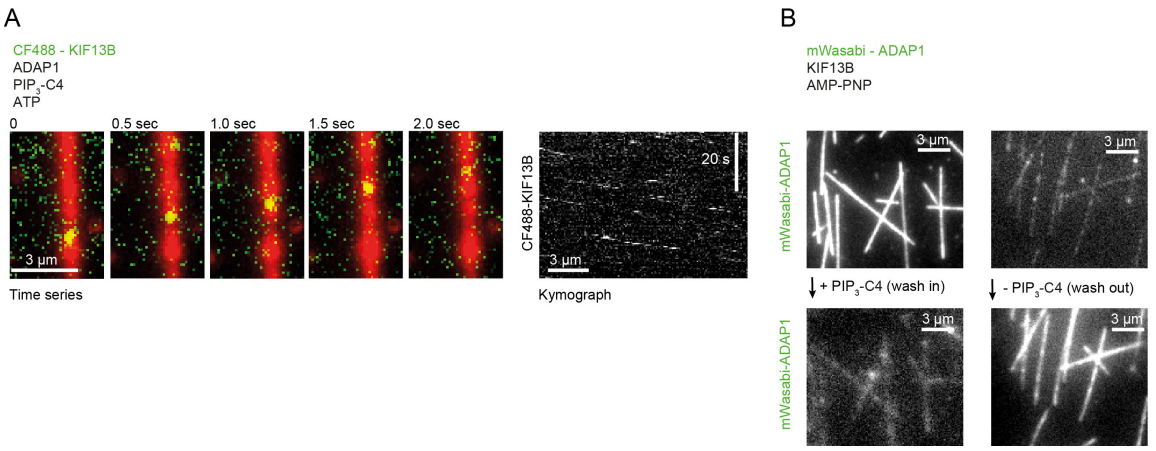

Figure S3: Control experiments related to Figure 2
(**A**) Left: Representative time series of CF_{488}-KIF13B single molecules (green, 10 nM) along HiLyte 647 microtubules (red) in the presence of 1 mM ATP, 100 nM unlabeled ADAP1 and washed-in water soluble PIP_3-C4 (23 µM). Right: Corresponding kymograph of the CF488 channel (right) showing that KIF13B remains motile after PIP_3-C4 has displaced ADAP1 from it. (**B**) Representative TIRF images of the mWasabi channel of PIP_3-C4 wash-in experiments (left) and PIP_3-C4 wash-out experiments (right) demonstrating reversible binding of mWasabi-ADAP1. For each assay type, the same field of view is depicted. Concentrations were: 160 nM mWasabi-ADAP1, 200 nM unlabeled KIF13B, 0.5 mM AMP-PNP and 23 µM water soluble PIP_3-C4 when indicated.

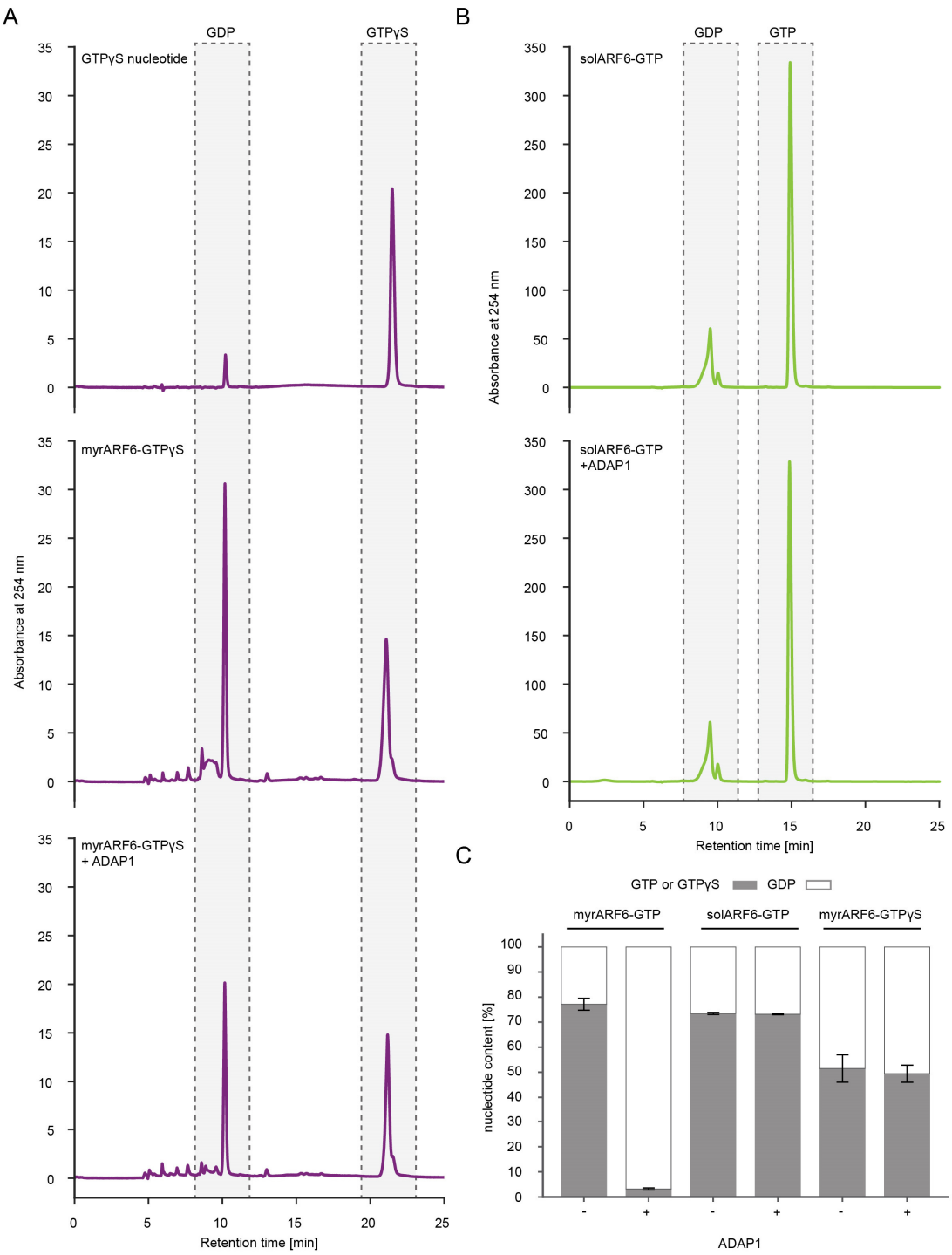

Figure S4: ADAP1 stimulated GAP activity requires lipid modified ARF6-GTP as substrate
(**A**) Representative HPLC chromatograms of GTPγS nucleotide (85% pure, top) compared to nucleotides extracted from GTPγS loaded myrARF6 incubated with PIP_3 vesicles in the absence (middle) or presence of 2μM ADAP1 (bottom). (**B**) HPLC traces of ARF6-GTP without myristoylation (=solARF6) with PIP_3 vesicles in the absence (top) or presence (bottom) of 2 μM ADAP1. (**C**) Quantification of the nucleotide content extracted from ARF6 under the indicated conditions. Error bars are standard deviations.

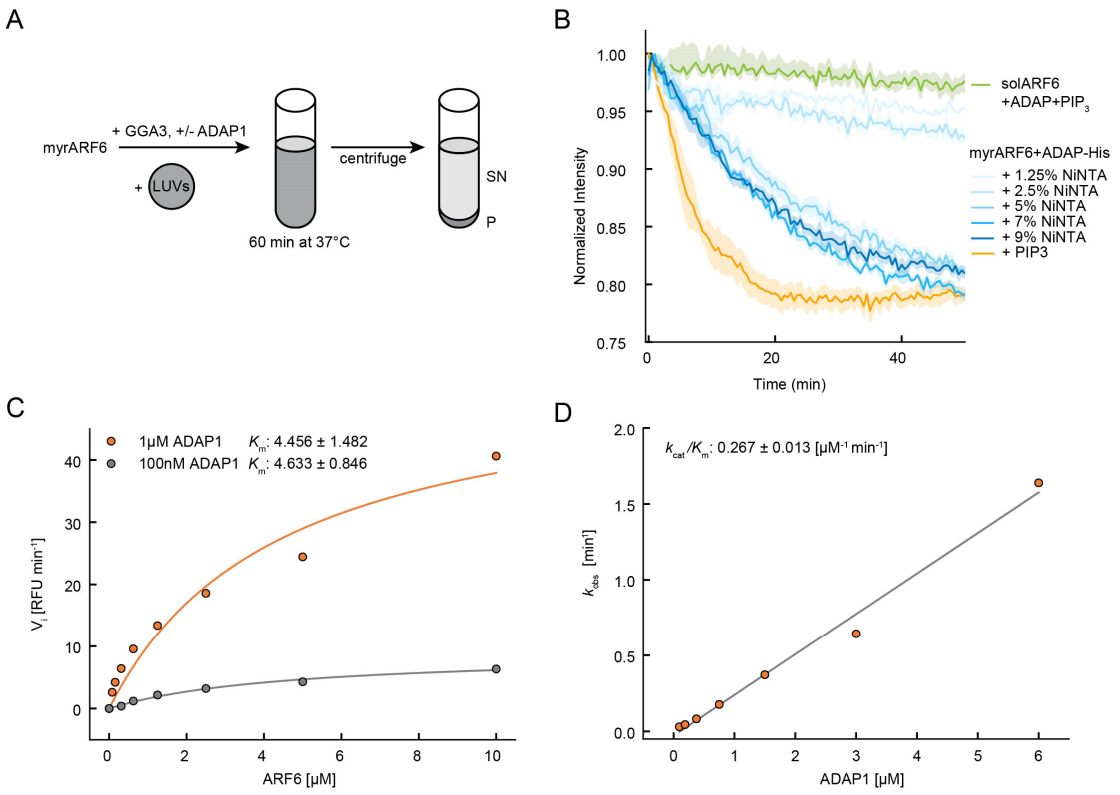

Figure S5: Enzyme characterization of ADAP1 and GAP activity of ADAP1-His in presence of NiNTA vesicles

(**A**) Scheme of end point GAP assay based on GGA3 recruitment to the vesicle pellet by ARF6 related to Fig. 4A. (**B**) Normalized tryptophan fluorescence of 4.5 µM myrARF6-GTP in the presence of 1.5 µM ADAP1-6xHis and 375 µM vesicles with the indicated amounts of NiNTA or 2.5 % PIP_3. Additionally, 4.5 µM soluble ARF6 in the presence of 1.5 µM ADAP1 and vesicles with 2.5 % PIP_3 was tested (green line). (**C**) Initial velocity values (V_i) of ADAP1 towards myrARF6-GTP dependent on increasing myrARF6-GTP concentrations (µM) shown in fluorescence decrease per time (RFUs/min). V_i values were measured for 1 µM ADAP1 (orange) and 100 nM ADAP1 (grey) and are fitted to a Michaelis-Menten equation (line) to extract K_m for 1 µM ADAP1 (4.46 (± 1.48)) and 100 nM ADAP1 (4.63 (± 0.85)). (**D**) k_{obs} (min^{-1}) values for different ADAP1 concentrations (µM) with a linear fit (line) to extract the catalytic efficiency k_{cat}/K_m of 0.27 (± 0.01) μM^{-1} min^{-1} from the slope. myrARF6-GTP concentration was 5.9 µM.

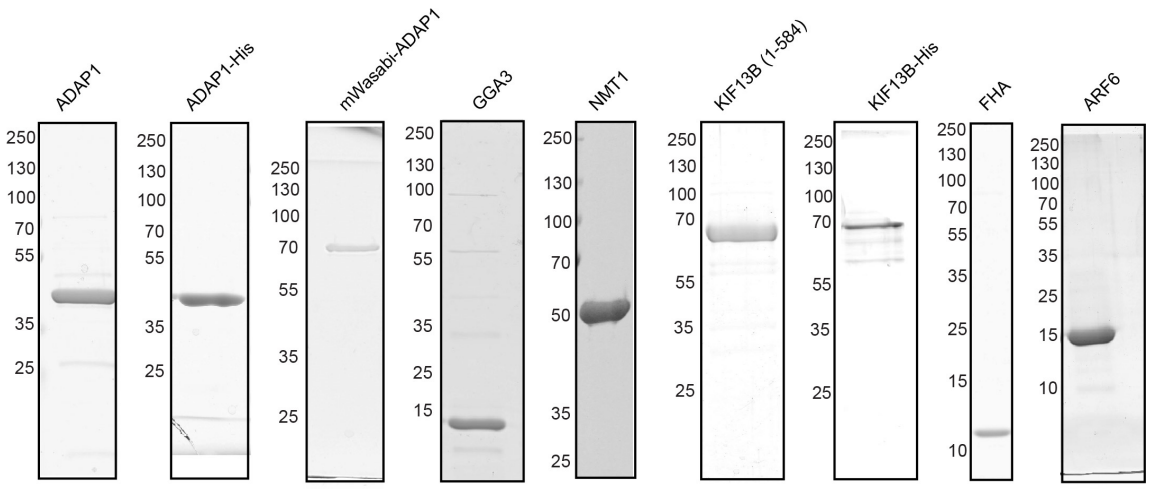

Figure S6: Purity of proteins used in this study
Purity of proteins used in this study documented by SDS page and CBB staining.

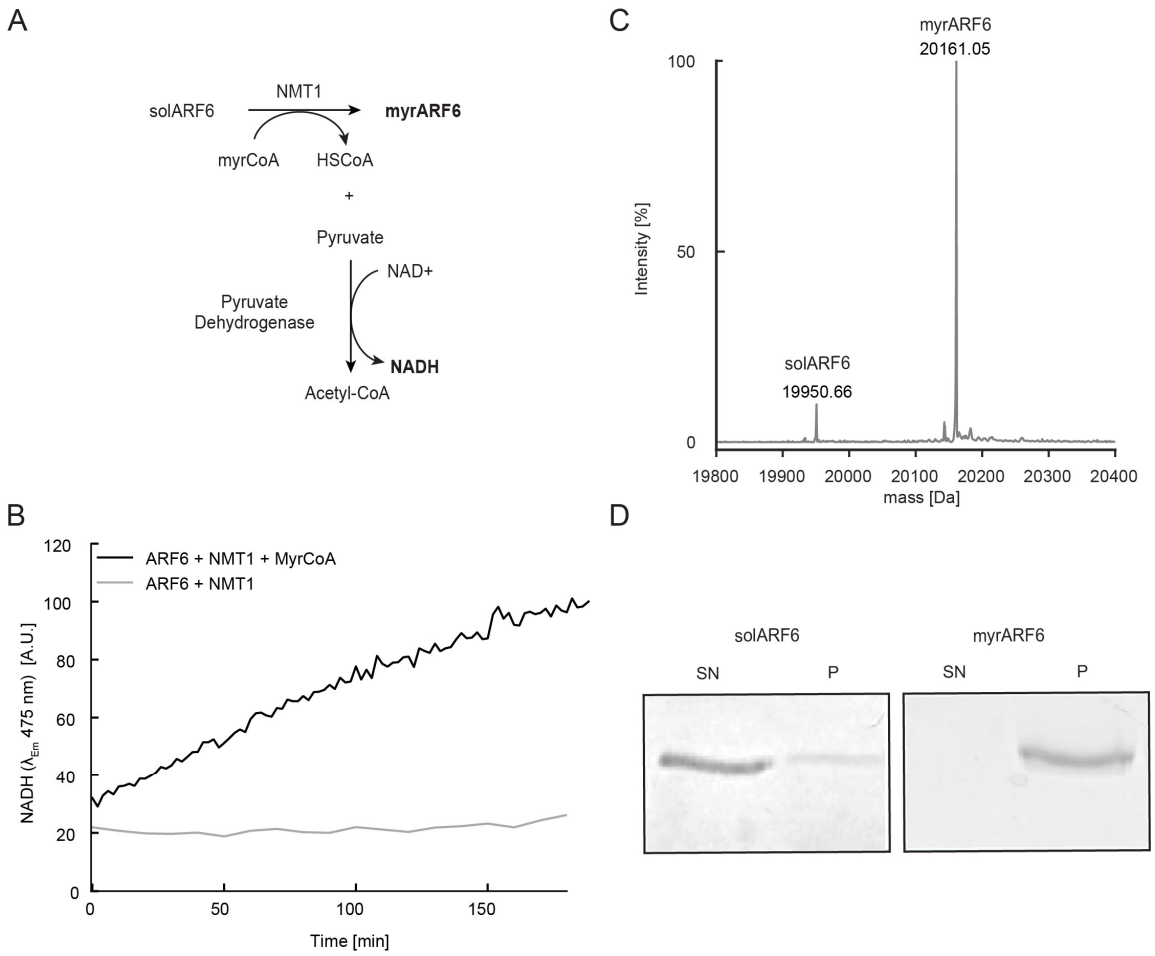

Figure S7: Production of ARF6 by *in vitro* myristoylation with NMT1.
(**A**) Scheme of real time monitoring of NMT1 mediated myristoylation of ARF6. The production of myrARF6 is coupled to the reduction of NAD+ to NADH resulting in increased fluorescence at 340 nm. (**B**) Time course of NADH fluorescence with NMT1 and ARF6 in the absence (grey) or presence (black) of myr-CoA. **(C)** Intact mass spectrometry confirmation of myristoylation: The dominant peak matches well with the expected mass for myrARF6 of 21,161.1 Da. (**D**) Vesicle sedimentation assay before (left) and after (right) myristoylation of ARF6-GTP. The absence of non-vesicle bound ARF6 after myristoylation indicates that the reaction was essentially complete. See methods for details.

Supplementary table 1: Summary of p-values from statistical tests

Panel	Conditions compared	Sample size	p value	Significance level
Fig. 1 D	"NTA vesicles + KIF13B-His" *vs* "PI(3,4,5)P_3 vesicles + ADAP1 and KIF13B"	12:12	5.9536E-09	***
Fig. 1 H	"no PI(3,4,5)P_3" *vs* with "PI(3,4,5)P_3"	10:10	0.00026	***
Fig. 2 B	"Control (ADAP1 alone)" *vs* "with KIF13B"	51:52	5.087E-25	***
Fig. 2 B	"with KIF13B" *vs* "with KIF13B and IP4"	52:50	9.522E-51	***
Fig. 2 B	"with KIF13B" *vs* "with KIF13B and PI(3,4,5)P_3"	52:41	1.581E-41	***
Fig. 2 B	"with KIF13B" *vs* "with KIF13B and PI(4,5P)$_2$"	52:51	0.02816185	*
Fig. 2 B	"with KIF13B" *vs* "with KIF13B and PI(3,4P)$_2$"	52:40	3.2403E-35	***
Fig. 2 C	"no PI(3,4,5)P_3" *vs* "with PI(3,4,5)P_3"	28:28	0.45812445	N.S.
Fig. 2 D[1]	"No PI(3,4,5)P_3" *vs* "after PI(3,4,5)P_3 wash in"	22:22	5.7069E-12	***
Fig. 4 A	GGA3 in pellet: "With ARF6-GTP" *vs* "with ARF6-GDP"	3:4	0.000508819	***
Fig. 4 A	GGA3 in pellet: "ARF6-GTP without ADAP1" *vs* "ARF6-GTP with ADAP1"	2:3	0.001722711	**
Fig. 4 A	GGA3 in pellet: "ARF6-GTP without ADAP1" *vs* "ARF6-GTPγS with ADAP1"	2:2	0.214061833	N.S.
Fig. 4 A	ARF6 in solution: "with ARF6-GTP" *vs* "with ARF6-GDP"	3:4	1.31467E-06	***
Fig. 4 A	ARF6 in solution: "ARF6-GTP without ADAP1" *vs* "ARF6-GTP with ADAP1"	2:3	0.012467034	*
Fig. 4 A	ARF6 in solution: "ARF6-GTP without ADAP1" *vs* "ARF6-GTPγS with ADAP1"	2:2	0.687890274	N.S.
Fig. 4 C/ Fig. S4C	"myrARF6-GTP without ADAP1" *vs* "myrARF6-GTP with ADAP1"	3:3	7.581E-07	***
Fig. S2 A	ADAP1 distribution: "no microtubules" *vs* "with microtubules"	3:3	0.00431067	**
Fig. S2 A	KIF13B distribution: "no microtubules" *vs* "with microtubules"	3:3	0.00032156	***
Fig. S2 B	ADAP1 distribution: "no PI(3,4,5)P_3 vesicles" *vs* "with PI(3,4,5)P_3 vesicles "	2:2	7.13025E-05	***
Fig. S2 B	KIF13B distribution: "no vesicles and no ADAP1" *vs* "with vesicles and with ADAP1"	3:3	0.49499353	N.S.
Fig. S2 B	KIF13B distribution: "with vesicles" *vs* "no vesicles"	3:3	0.57565209	N.S.

Fig. S2 B	KIF13B distribution with vesicles: “no ADAP1” *vs* “with ADAP1”	3:3	0.29397027	N.S.
Fig. S4 A	“myrARF6-GTPγS without ADAP1” *vs* “myrARF6-GTPγS with ADAP1”	2:2	0.98	N.S.
Fig. S4 B	“solARF6-GTP without ADAP1” *vs* “solARF6-GTP with ADAP1”	3:3	0.31	N.S.

N.S: Not significant, * : $p < 0.05$, ** : $p < 0.01$ and *** $p < 0.001$.
1: For this data set, a paired t test was used

Supplementary movie legends

Movie S1: Confirmation of KIF13B motor activity by microtubule gliding
Movie S1, related to SI Appendix Fig. S1 D. Paclitaxel stabilized Hilyte647 microtubules are transported by glass coverslip adsorbed unlabeled KIF13B molecules in the presence of ATP. Time is in seconds.

Movie S2: ADAP1 and KIF13B do not transport PIP_3 vesicles
Movie S2, related to Fig. 1C. Time lapse movie of Rhodamine labeled PIP_3 vesicles (yellow, 5 mol %) above HiLyte647 microtubules (blue) in the presence of 500 nM KIF13B and 500 nM ADAP1 (right). Time is in seconds.

Movie S3: Vesicle transport by KIF13B-6xHis
Movie S3, related to Fig. 1C. Time lapse movie of Rhodamine labeled NTA vesicles (yellow, 3 mol % Ni-NTA) above HiLyte647 microtubules (blue) in the presence of 500 nM KIF13B-6xHis. Time is in seconds

Movie S4: PIP_3 inhibits KIF13B mediated transport of ADAP1
Movie S3, related to Fig. 1G. Fluorescent signals of 20 nM mWasabi-ADAP1 (yellow) above Hilyte 647 microtubules (blue) with 100 nM unlabeled KIF13B in the absence (left) or presence (right) of 23 µM water soluble PIP_3-C4. ATP was present in both conditions at 1 mM. Time is in seconds.

SI References

1. H. W. Ai, S. G. Olenych, P. Wong, M. W. Davidson, R. E. Campbell, Hue-shifted monomeric variants of Clavularia cyan fluorescent protein: Identification of the molecular determinants of color and applications in fluorescence imaging. *BMC Biol.* **6**, 1–13 (2008).
2. C. Duellberg, *et al.*, Reconstitution of a hierarchical +TIP interaction network controlling microtubule end tracking of dynein. *Nat. Cell Biol.* **16** (2014).
3. K. H. Yamada, T. Hanada, A. H. Chishti, The effector domain of human Dlg tumor suppressor acts as a switch that relieves autoinhibition of kinesin-3 motor GAKIN/KIF13B. *Biochemistry* **46**, 10039–10045 (2007).
4. B. Hall, *et al.*, A fluorescence resonance energy transfer activation sensor for Arf6. *Anal. Biochem.* (2008) https:/doi.org/10.1016/j.ab.2007.11.032.
5. B. Boisson, T. Meinnel, A continuous assay of myristoyl-CoA:protein N-myristoyltransferase for proteomic analysis. *Anal. Biochem.* (2003) https:/doi.org/10.1016/j.ab.2003.07.007.
6. D. Padovani, M. Zeghouf, J. A. Traverso, C. Giglione, J. Cherfils, High yield production of myristoylated Arf6 small GTPase by recombinant N-myristoyl transferase. *Small GTPases* (2013) https:/doi.org/10.4161/sgtp.22895.
7. C. S. Theile, *et al.*, Site-specific N-terminal labeling of proteins using sortase-mediated reactions. *Nat. Protoc.* (2013) https:/doi.org/10.1038/nprot.2013.102.
8. S. B. Nielsen, D. E. Otzen, Quartz crystal microbalances as tools for probing protein-membrane interactions. *Methods Mol. Biol.* (2013) https:/doi.org/10.1007/978-1-62703-275-9_1.
9. P. Bieling, I. A. Telley, C. Hentrich, J. Piehler, T. Surrey, *Fluorescence microscopy assays on chemically functionalized surfaces for quantitative imaging of microtubule, motor, and +tip dynamics* (2010) https:/doi.org/10.1016/S0091-679X(10)95028-0.
10. M. Trokter, N. Mucke, T. Surrey, Reconstitution of the human cytoplasmic dynein complex. *Proc. Natl. Acad. Sci.* (2012) https:/doi.org/10.1073/pnas.1210573110.